Theory of phonon-modulated electron spin relaxation time based on the projection–reduction method

Nam Lyong Kang[a)†] and Sang Don Choi[b)]

[a)] *Department of Applied Nanoscience, Pusan National University, Miryang* 627-706, *Republic of Korea*
[b)] *Department of Physics, Kyungpook National University, Daegu* 702-701, *Republic of Korea*

(Received 10 January 2014; revised manuscript received 20 February 2014; published online 10 June 2014)

This paper introduces a new method for a formula for electron spin relaxation time of a system of electrons interacting with phonons through phonon-modulated spin–orbit coupling using the projection–reduction method. The phonon absorption and emission processes as well as the photon absorption and emission processes in all electron transition processes can be explained in an organized manner, and the result can be represented in a diagram that can provide intuition for the quantum dynamics of electrons in a solid. The temperature (T) dependence of electron spin relaxation times (T_1) in silicon is $T_1 \propto T^{-1.07}$ at low temperatures and $T_1 \propto T^{-3.3}$ at high temperatures for acoustic deformation constant $P_{\rm ad} = 1.4 \times 10^7$ eV and optical deformation constant $P_{\rm od} = 4.0 \times 10^{17}$ eV/m. This means that electrons are scattered by the acoustic deformation phonons at low temperatures and optical deformation phonons at high temperatures, respectively. The magnetic field (B) dependence of the relaxation times is $T_1 \propto B^{-2.7}$ at 100 K and $T_1 \propto B^{-2.3}$ at 150 K, which nearly agree with the result of Yafet, $T_1 \propto B^{-3.0} \sim B^{-2.5}$.

Keywords: electron spin resonance, spin–orbit coupling, projection–reduction method, phonon scattering

PACS: 71.70.Ej, 72.25.Rb, 85.75.−d **DOI:** 10.1088/1674-1056/23/8/087102

1. Introduction

In recent years, a study of electron spin has attracted considerable attention in quantum computation and spintronics application. The electron spin might find application in the future to create new logic devices capable of lower power consumption and higher performance.[1–8] Silicon is a very suitable host material for fabricating spintronics devices because it has low atomic weight, lattice inversion symmetry, and relatively long spin relaxation time due to the weak spin–orbit interaction and poor electron–nuclear spin coupling.[9–13] Electron spin resonance (ESR)[14–18] is a promising technique for measuring the spin relaxation time because the absorption lineshapes are sensitive to the type of scattering mechanisms affecting the carrier behavior. The main scattering mechanisms that affect the spin relaxation are due to phonons, ionized impurities, other carriers, and interface roughness. Among them, the electron–phonon interaction is the dominant process in relatively pure semiconductors.

The main spin relaxation mechanism at high temperatures is generally considered to be the Elliott–Yafet mechanism mediated through spin–orbit coupling.[19,20] While spin flips are due to phonon-modulated spin–orbit coupling in the Yafet processes,[20] in the Elliott processes,[19] they are due to the admixture of the Pauli up and down spins caused by spin–orbit coupling. Since Yafet reported that the inclusion of the Yafet term in the electron–phonon coupling function is essential for obtaining the correct temperature dependence of the relaxation time, considerable research interest has been focused on this area.[20–25] Although the temperature dependence of the relaxation time might be caused by the Planck and Fermi distribution functions, the relaxation times[21–25] obtained using the density functional perturbation theory or pseudopotential model have limited applications, because the two distribution functions are simply added (or subtracted) or the Fermi distribution function is not contained, such as $N_q + 1/2 \mp 1/2 \pm f_\alpha$ or $N_q + 1/2 \pm 1/2$, where N_q and f_α are the Planck distribution function for a phonon with wave vector q and the Fermi distribution function for an electron with energy E_α, respectively. In spintronics, preserving the information injected into a spin over a practical time scale is important for the spintronics devices. Therefore, it is crucial to understand how the distribution functions are included because the temperature dependence of the spin relaxation time might be caused by the Planck and Fermi distribution functions.

Recently the present authors derived an ESR absorption lineshape function considering spin–orbit interaction[26] using the reduction identity and state-dependent projection technique, in which phonon-modulated spin–orbit coupling was not taken into consideration. More recently, the authors showed that the proper combination of state-dependent projectors and reduction identities could produce the lineshape formula satisfying the population criterion as well as the energy conservation criterion.[27] We claim that a validated theory should satisfy the population criterion, which requires that the electron and phonon distributions should be included in the expression in multiplicative form properly for each transition process. Furthermore, the formulae derived by using this new method, later coined the "projection–reduction method

†Corresponding author. E-mail: nlkang@pusan.ac.kr

© 2014 Chinese Physical Society and IOP Publishing Ltd

(PR method)", was shown to be represented by Feynman-like diagrams.[28] In this paper, a new formula for the electron spin relaxation time for a system of electrons interacting with phonons through phonon-modulated spin–orbit coupling will be derived using the PR method. An explicit expression including the electron and phonon distribution functions will be given properly. Therefore, the absorption and emission processes of phonons and photons in all electron transition processes can be explained in an organized manner, and the result can be represented in a diagram that can provide intuition for the quantum dynamics of electrons in a solid. The formula will be applied to obtaining the temperature and magnetic field dependence of relaxation times for silicon and the numerical results will be compared with those obtained by Yafet[20] and Huang *et al.*[29]

2. Preliminaries

2.1. Electron spin–lattice relaxation time

When electrons in a semiconductor are transferred from lower energy states to higher energy states by absorbing electromagnetic radiation, the system, as is left out of equilibrium, must undergo reverse transitions to get back to equilibrium. This process, called "spin–lattice relaxation", is mostly characterized by electron–phonon interaction in the semiconductor.

Experimentally, this process is measured in terms of the characteristic time called the spin–lattice relaxation time denoted by T_1. Theoretically, T_1 can be expressed as a function of the lineshape function $\Gamma(\omega)$, ω being the angular frequency of the electromagnetic wave, as[30]

$$\hbar/T_1 = 2\mathrm{Im}\{\Gamma(\omega)\}, \tag{1}$$

where Im means "the imaginary part of". Note that $\Gamma(\omega)$ is contained in the (Lorentziation-like form of) absorption power $P(\omega)$, which is proportional to the real part of the optical magnetic susceptibility tensor $\chi(\omega)$ in the susceptibility formalism.

2.2. Magnetic susceptibility and lineshape function based on the projection–reduction method

When an electromagnetic wave with angular frequency ω is applied to a system along the z direction, the magnetic susceptibility tensor can be defined as[26,31]

$$\chi_{+-}(\omega) = -\frac{g^2\mu_B^2}{2\Omega_0}\mathrm{Im}\left[\sum_\alpha \bar{\chi}^{(\alpha)}_{+-}(\omega)\right]. \tag{2}$$

Here, g is the electron g-factor, μ_B the Bohr magneton, Ω_0 the volume of the system and

$$\bar{\chi}^{(\alpha)}_{+-}(\omega) \equiv \mathrm{Tr}\left\{\rho_{eq}[(\hbar\bar{\omega} - L_{eq})^{-1}\sigma_+, a^\dagger_{\alpha-}a_{\alpha+}]\right\}, \tag{3}$$

where Tr denotes the many-body trace, ρ_{eq} the equilibrium density operator, $\bar{\omega} \equiv \omega - \mathrm{i}a\,(a \to 0^+)$, σ the Pauli spin matrix, L_{eq} is the Liouville operator corresponding to the equilibrium Hamiltonian H_{eq} defined as $L_{eq}X = H_{eq}X - XH_{eq}$ for an arbitrary operator X, and $a^\dagger_{\alpha,s_\alpha}(a_{\alpha,s_\alpha})$ is the creation (annihilation) operator for an electron in the state $|\alpha, s_\alpha\rangle$ with spin s_α and energy E_{α,s_α}. L_{eq} can be split as $L_{eq} = L_d + L_v$ for calculation convenience, where L_d and L_v are the Liouville operators corresponding to the unperturbed Hamiltonian $H_d = H_e + H_p$ and the perturbed Hamiltonian V, H_e and H_p being the electron and phonon Hamiltonians, respectively.

To calculate Eq. (3), the state-dependent projection operators for an arbitrary operator X are introduced as follows:

$$PX = \frac{\langle X\rangle_\alpha}{\langle\sigma_+\rangle_\alpha}\sigma_+, \quad Q = 1 - P, \tag{4}$$

where

$$\langle X\rangle_\alpha \equiv \mathrm{Tr}\left\{\rho_{eq}[X, a^\dagger_{\alpha-}a_{\alpha+}]\right\}. \tag{5}$$

Note that the projection operators given in Eq. (4) are state-dependent because they depend on the $\alpha+$ and $\alpha-$ states. After a procedure similar to that for Eq. (3.11) in Ref. [26], we obtain

$$\bar{\chi}^{(\alpha)}_{+-}(\bar{\omega}) = \frac{\langle\sigma_+\rangle_\alpha}{\hbar\bar{\omega} - E_{+-} - \Gamma_\alpha(\bar{\omega})} \tag{6}$$

where the lineshape function, $\Gamma_\alpha(\bar{\omega})$, is given as follows:

$$\Gamma_\alpha(\bar{\omega})\langle\sigma_+\rangle_\alpha \equiv \langle L_v\sigma_+\rangle_\alpha + \langle L_{eq}Q(\hbar\bar{\omega} - L_{eq}Q)^{-1}L_v\sigma_+\rangle_\alpha. \tag{7}$$

The approximation, $\rho_{eq}(H) \approx \rho_{eq}(H_e)$, can be used, assuming that the spin–orbit interaction is quite weak. The first term in Eq. (7) can then be neglected because the averages of b_q and $b^\dagger_q$ are zeros and the second term can be calculated using the first-kind of Kang–Choi reduction identity given by[26,27] $\mathrm{Tr}\{\rho_{eq}[L_{eq}X, A]\} = -\mathrm{Tr}\{\rho_{eq}[X, L_{eq}A]\}$ for the arbitrary operators X and A, which can be obtained using the fact that $\rho_{eq}(H)$ commutes with H and $\mathrm{Tr}(ABC) = \mathrm{Tr}(BCA)$. Applying it to the second term in Eq. (7) and using $\mathrm{Tr}\{\rho_{eq}[Q(\hbar\bar{\omega} - L_{eq}Q)^{-1}L_v\sigma_+, a^\dagger_{\alpha-}a_{\alpha+}]\} = 0$, we have

$$\Gamma_\alpha(\bar{\omega})\langle\sigma_+\rangle_\alpha = \mathrm{Tr}\left\{\rho_{eq}\left[(\hbar\bar{\omega} - L_d)^{-1}L_v\sigma_+, L_v a^\dagger_{\alpha-}a_{\alpha+}\right]\right\} \tag{8}$$

in the second order approximation in L_v. Equation (8) is an easily calculable form because it contains neither L_v nor the projection operator in the operator denominator.

The denominator in Eq. (6) represents the transition from an initial state with down spin ($\alpha-$ state) to a final state with up spin ($\alpha+$ state) with a photon absorption of frequency ω and lineshape function $\Gamma_\alpha(\bar{\omega})$, which contains the effect of the spin–orbit interaction. If there is no spin–orbit interaction, the shape of the susceptibility would be like a delta function. On the other hand, the shape is broadened as electrons are scattered by the interaction, so $\Gamma_\alpha(\bar{\omega})$ is included. Implicit states

exist between the initial and final states because $\Gamma_\alpha(\bar{\omega})$ contains implicit transitions between the initial (or final) and implicit states by the spin–orbit interaction. An implicit state should be coupled with the initial (or final) state by a proper interaction coupling factor in the case of an implicit transition between the final (or initial) and implicit states. $\Gamma_\alpha(\bar{\omega})$ must also contain energy denominator factors enforcing the energy conservation in each implicit transition and population factors regulating the implicit transition.

3. System specified

3.1. Hamiltonian of the general system

For a system of electrons interacting with phonons through phonon-modulated spin–orbit coupling under a static magnetic field B applied along the z axis, the following equilibrium Hamiltonian is considered:

$$H_{\rm eq} = \sum_{\alpha,s_\alpha} E_{\alpha,s_\alpha} a^\dagger_{\alpha,s_\alpha} a_{\alpha,s_\alpha} + \sum_q \hbar\omega_q b^\dagger_q b_q + V. \tag{9}$$

Here, the first term is the electron Hamiltonian $H_{\rm e}$ including the Zeeman term, the second is the phonon Hamiltonian $H_{\rm p}$, V is the electron–phonon interaction Hamiltonian, which is defined later, and $b^\dagger_q(b_q)$ is the creation (annihilation) operator for a phonon in the state $|q\rangle$ with energy $\hbar\omega_q$, $|q\rangle \equiv |\boldsymbol{q}, l\rangle$, $\boldsymbol{q}$ is the phonon wave vector and l is the polarization index. E_{α,s_α} is the eigenvalue of the single electron Hamiltonian given as follows:

$$h_{\rm e} = \frac{1}{2m_{\rm e}}(\boldsymbol{p} + e\boldsymbol{A})^2 + g\mu_{\rm B}B\sigma_z/2, \tag{10}$$

where $\boldsymbol{p}$ is the momentum operator of an electron with the effective mass $m_{\rm e}$ and $\boldsymbol{A}$ is the vector potential.

If the Landau gauge, $\boldsymbol{A} = (0, Bx, 0)$, is adopted, the eigenvalue is given as follows:

$$E_{\alpha,s_\alpha} \equiv E_\alpha + E_{s_\alpha} = (n_\alpha + 1/2)\hbar\omega_c + \hbar^2 k^2_{z\alpha}/2m_{\rm l} + g\mu_{\rm B}Bs_\alpha/2, \tag{11}$$

where $n_\alpha = 0, 1, 2, \ldots$, $\omega_{\rm c} \equiv eB/m_{\rm t}$ is the cyclotron frequency, $k_{z\alpha}$ is the z component of the electron wave vector and $s_\alpha = +1\ (-1)$ for a spin up (down), and $m_{\rm t}\,(m_{\rm l})$ is the transverse (longitudinal) effective mass. The conduction band of silicon has many equivalent ellipsoidal energy surfaces in the first Brillouin zone. Therefore, there are two effective masses and the transverse (cyclotron) effective mass varies as the magnetic field direction changes. In this paper, however, we consider an intravalley process at the valley center and choose the spherically averaged effective mass $m_{\rm e} = (m_{\rm l} m^2_{\rm t})^{1/3}$. The eigenfunction is given as

$$\Psi_\alpha(\boldsymbol{r})\chi_{s_\alpha} = \frac{1}{\sqrt{L_y L_z}} {\rm e}^{{\rm i}k_y y + {\rm i}k_z z} \phi_{n_\alpha}(x)\chi_{s_\alpha}. \tag{12}$$

Here, L_y and L_z are the normalization lengths, χ_{s_α} is the spinor for a spin s_α and $\phi_n(x)$ is the harmonic oscillator wave function given as

$$\phi_n(x) = (m_{\rm e}\omega_{\rm c}/\hbar\pi)^{1/4}(2^n n!)^{-1/2} \times \exp\left[-(x - x_{\rm c})^2/2r_0^2\right] {\rm H}_n\left[(x - x_{\rm c})/r_0\right]$$

where $x_{\rm c} \equiv -hk_y/eB$, $r_0 \equiv (\hbar/eB)^{1/2}$ and ${\rm H}_n(x)$ is the Hermite polynomial.

3.2. Perturbation

In this paper, the phonon-modulated spin–orbital interaction Hamiltonian given by the following equation is considered as the perturbed Hamiltonian:[20–22]

$$V = \frac{\hbar}{4m^2_{\rm e}c^2}[\nabla V_{\rm ep} \times (\boldsymbol{p} + e\boldsymbol{A})] \cdot \boldsymbol{\sigma}. \tag{13}$$

Here, c is the speed of light and $V_{\rm ep}$ is the deformation potential, which is assumed to be proportional to the gradient of displacement for acoustic mode, $\boldsymbol{u}$, given by

$$\boldsymbol{u} = \sum_q \sqrt{\frac{\hbar}{2\rho_{\rm m}\Omega_0\omega_q}}(b_q + b^\dagger_{-q}) {\rm e}^{{\rm i}\boldsymbol{q}\cdot\boldsymbol{r}} \hat{e}_q, \tag{14}$$

where $\rho_{\rm m}$ is the mass density and $\hat{e}_q$ is the polarization vector, i.e., we consider the following deformation potential for acoustic mode:[32]

$$V_{\rm ep} = P_{\rm ad} \nabla \cdot \boldsymbol{u}, \tag{15}$$

where $P_{\rm ad}$ is the acoustic deformation constant, which will be used as a parameter. In contrast to the case of acoustic vibrations where the electron–phonon interaction potential is proportional to the derivative of the atomic displacement, the deformation potential for the optical mode is assumed to be proportional to the atomic displacement,[32] i.e.

$$V_{\rm ep} = P_{\rm od} u \tag{16}$$

is chosen, where $P_{\rm od}$ is an optical deformation constant. It should be noted that the temperature dependence of the spin relaxation time (or linewidth) is affected by neither $P_{\rm ad}$ nor $P_{\rm od}$ because they are not contained in the distribution functions for electrons and phonons. These two constants only affect the magnitude of the relaxation time. In this paper, we used the two constants as fitting parameters.

Equation (13) can be written in the following second quantized form:

$$V = \sum_{j=x,y,z} \sum_{\alpha,\beta} \sum_{s_\alpha, s_\beta} \sum_q [l_j(q)]_{\alpha\beta} a^\dagger_{\beta,s_\beta} a_{\alpha,s_\alpha} (b_q + b^\dagger_{-q})(\chi_{s_\alpha} \sigma_j \chi_{s_\beta}). \tag{17}$$

Here, $(X)_{\alpha\beta} \equiv \int {\rm d}\boldsymbol{r} \Psi^*_\alpha(\boldsymbol{r}) X \Psi_\beta(\boldsymbol{r})$ and

$$\boldsymbol{l}(q) \equiv \frac{\hbar D_q}{4m^2_{\rm e}c^2}[\nabla {\rm e}^{{\rm i}\boldsymbol{q}\cdot\boldsymbol{r}} \times (\boldsymbol{p} + e\boldsymbol{A})], \tag{18}$$

where $D_q \equiv {\rm i}P_{\rm ad} q\sqrt{\hbar/2\rho_{\rm m}\Omega_0\omega_q}$ for the acoustic mode and $D_q \equiv P_{\rm od}\sqrt{\hbar/2\rho_{\rm m}\Omega_0\omega_q}$ for the optical mode.

Using the Pauli spin matrices, equation (17) can be expressed as follows:

$$V=\sum_{\alpha,\beta}\sum_{q}\sum_{j}[l_j(q)]_{\alpha\beta}s^{j}_{\alpha\beta}(b_q+b^{\dagger}_{-q}), \tag{19}$$

where the $s^{j}_{\alpha\beta}$ can be expressed as: $s^{x}_{\alpha\beta}\equiv a^{\dagger}_{\alpha+}a_{\beta-}+a^{\dagger}_{\alpha-}a_{\beta+}$, $s^{y}_{\alpha\beta}\equiv -\mathrm{i}a^{\dagger}_{\alpha+}a_{\beta-}+\mathrm{i}a^{\dagger}_{\alpha-}a_{\beta+}$, and $s^{z}_{\alpha\beta}\equiv a^{\dagger}_{\alpha+}a_{\beta+}-a^{\dagger}_{\alpha-}a_{\beta-}$.

4. Derivation of formulae

4.1. Lineshape function

To calculate Eq. (8), we make use of the following equations:

$$\begin{aligned}(\hbar\bar{\omega}-L_{\mathrm{d}})^{-1}L_{\mathrm{v}}\sigma_{+} &= 2\sum_{\alpha,\beta}\sum_{q}\Big\{[l_z(q)]_{\alpha\beta}G^{(-+)}_{\beta\alpha}(+\omega_q)b_q s^{\dagger}_{\alpha\beta}\\ &+[l_z(q)]_{\alpha\beta}G^{(-+)}_{\beta\alpha}(-\omega_q)b^{\dagger}_{-q}s^{\dagger}_{\alpha\beta}\\ &-[l^{\dagger}(q)]_{\alpha\beta}G^{(\mathrm{c})}_{\beta\alpha}(+\omega_q)b_q s^{z}_{\alpha\beta}\\ &-[l^{\dagger}(q)]_{\alpha\beta}G^{(\mathrm{c})}_{\beta\alpha}(-\omega_q)b^{\dagger}_{-q}s^{z}_{\alpha\beta}\Big\}, \end{aligned}\tag{20}$$

$$\begin{aligned}L_{\mathrm{v}}a^{\dagger}_{\alpha-}a_{\alpha+} &= \sum_{\gamma}\sum_{q}(b_q+b^{\dagger}_{-q})\Big\{[l^{-}(q)]_{\gamma\alpha}a^{\dagger}_{\gamma+}a_{\alpha+}\\ &-[l^{-}(q)]_{\alpha\gamma}a^{\dagger}_{\alpha-}a_{\gamma-}-[l_z(q)]_{\alpha\gamma}a^{\dagger}_{\alpha-}a_{\gamma+}\\ &-[l_z(q)]_{\gamma\alpha}a^{\dagger}_{\gamma-}a_{\alpha+}\Big\}, \end{aligned}\tag{21}$$

where $l^{\pm}\equiv l_x\pm\mathrm{i}l_y$, $[l_z(q)]_{\alpha\beta}$ and $[l^{\pm}(q)]_{\alpha\beta}$ are called the interaction coupling factors, and the two energy denominator factors are defined as follows:

$$G^{(-+)}_{\beta\alpha}(\pm\omega_q)\equiv(\hbar\bar{\omega}+E_{\beta-}-E_{\alpha+}\pm\omega_q)^{-1}, \tag{22}$$

which corresponds to a spin flip process, and

$$G^{(\mathrm{c})}_{\beta\alpha}(\pm\omega_q)\equiv(\hbar\bar{\omega}+E_{\beta}-E_{\alpha}\pm\omega_q)^{-1}, \tag{23}$$

which corresponds to a spin conserving process.

In Eqs. (6)–(8), $\langle\sigma_{+}\rangle_{\alpha}$ can be calculated as follows:

$$\langle\sigma_{+}\rangle_{\alpha}\equiv\mathrm{Tr}\Big\{\rho[\sigma_{+},a^{\dagger}_{\alpha-}a_{\alpha+}]\Big\}=2(f_{\alpha+}-f_{\alpha-}), \tag{24}$$

where $f_{\alpha+}$ ($f_{\alpha-}$) is the Fermi distribution function for an electron in the state $|\alpha\rangle$ with an up (down) spin. Therefore, inserting Eqs. (20), (21), and (24) into Eq. (8), and considering $\lim_{a\to 0^{+}}(x-\mathrm{i}a)^{-1}=P(1/x)+\mathrm{i}\pi\delta(x)$ where P denotes the Cauchy principal value, we have

$$\chi_{+-}(\omega)=\frac{g^2\mu_{\mathrm{B}}^2}{\Omega_0}\sum_{\alpha}\frac{(f_{\alpha-}-f_{\alpha+})\mathrm{Im}\{\Gamma_{\alpha}(\omega)\}}{[\hbar\omega-E_{+-}-\mathrm{Re}\{\Gamma_{\alpha}(\omega)\}]^2+[\mathrm{Im}\{\Gamma_{\alpha}(\omega)\}]^2}. \tag{25}$$

Here, the linewidth, $\mathrm{Im}\{\Gamma_{\alpha}(\bar{\omega})\}$, is given as

$$\begin{aligned}&\mathrm{Im}\{\Gamma_{\alpha}(\bar{\omega})\}(f_{\alpha-}-f_{\alpha+})\\ &=\pi\sum_{\gamma}\sum_{q}\Big\{2|[l_z(q)]_{\gamma\alpha}|^2\Delta^{(-+)}_{\alpha\gamma}(+\omega_q)P^{(-+)}_{\alpha\gamma}\\ &+2|[l_z(q)]_{\alpha\gamma}|^2\Delta^{(-+)}_{\gamma\alpha}(+\omega_q)P^{(-+)}_{\gamma\alpha}\\ &-2|[l_z(q)]_{\gamma\alpha}|^2\Delta^{(-+)}_{\alpha\gamma}(-\omega_q)P^{(+-)}_{\gamma\alpha}\\ &-2|[l_z(q)]_{\alpha\gamma}|^2\Delta^{(-+)}_{\gamma\alpha}(-\omega_q)P^{(+-)}_{\alpha\gamma}\\ &+|[l^{+}(q)]_{\alpha\gamma}|^2\Delta^{(\mathrm{c})}_{\gamma\alpha}(+\omega_q)P^{(++)}_{\gamma\alpha}\\ &+|[l^{+}(q)]_{\gamma\alpha}|^2\Delta^{(\mathrm{c})}_{\alpha\gamma}(+\omega_q)P^{(--)}_{\alpha\gamma}\\ &-|[l^{+}(q)]_{\alpha\gamma}|^2\Delta^{(\mathrm{c})}_{\gamma\alpha}(-\omega_q)P^{(++)}_{\alpha\gamma}\\ &-|[l^{+}(q)]_{\gamma\alpha}|^2\Delta^{(\mathrm{c})}_{\alpha\gamma}(-\omega_q)P^{(--)}_{\gamma\alpha}\Big\}\\ &=A+B+C+D+E+F+G+H, \end{aligned}\tag{26}$$

where $|[\boldsymbol{l}(q)]_{\alpha\beta}|^2\equiv[\boldsymbol{l}(q)]_{\alpha\beta}\times[\boldsymbol{l}(-q)]_{\beta\alpha}$, $\Delta^{(-+)}_{\beta\alpha}(\pm\omega_q)\equiv\delta(\hbar\omega+E_{\beta-}-E_{\alpha+}\pm\hbar\omega_q)$, and $\Delta^{(\mathrm{c})}_{\beta\alpha}(\pm\omega_q)\equiv\delta(\hbar\omega+E_{\beta}-E_{\alpha}\pm\hbar\omega_q)$ are Dirac delta functions, through which the energy conservation is maintained, and the population factor is defined as

$$P^{(ss')}_{\alpha\beta}\equiv N_q f_{\alpha s}(1-f_{\beta s'})-(1+N_q)f_{\beta s'}(1-f_{\alpha s}), \tag{27}$$

where N_q is the Planck distribution function for a phonon with energy $\hbar\omega_q$. Equation (27) means a transition from an (α,s) state to a (β,s') state with phonon absorption (N_q) minus a transition from a (β,s') state to an (α,s) state with phonon emission $(1+N_q)$.

Although $\Gamma_{\alpha}(\bar{\omega})$ is called the lineshape function, the lineshape must be calculated from Eq. (25) and not directly from Eq. (26). Equation (26) can explain the spin flip and conserved processes properly (Fig. 1) because it contains the distribution functions for electrons and phonons in multiplicative forms [see Eq. (27)]. Note that the population differences do not appear properly in the result of Kawabata [Ref. [31]]. The relaxation time can be calculated directly from Eq. (26) if the Lorentzian approximation is assumed for the weak phonon scattering. Equation (26) can be represented by the diagram in Fig. 1. The first four terms (vertical red solid arrows) correspond to spin flip processes, and the other four terms (vertical green dotted arrows) correspond to the spin conserving processes. The red and green arrows pointing upward (downward) correspond to the photon absorption (emission) processes and the horizontal blue dotted arrows pointing to (outward from) the vertical red and green arrows correspond to phonon absorption (emission) processes.

The physical meaning of Eq. (26) is as follows. The first term, which is a spin flip process (A in Fig. 1), corresponds to an implicit transition between the initial state with a down spin ($\alpha-$ state) and an implicit state with an up spin ($\gamma+$ state). The states given by γ are called implicit states because they are included only in the lineshape function [Eq. (26)], not in susceptibility [Eq. (25)]. $P^{(-+)}_{\alpha\gamma}$ means that a reverse implicit transition from the implicit up-spin state to the initial down-spin state with photon and phonon emission should be subtracted from the forward implicit transition from the initial state to the implicit state with photon and phonon absorption. This

means that when an electron–phonon interaction is involved in an electron transition, the electron undergoes an implicit transition from the initial state to the implicit state (and *vice versa*) with photon absorption (emission) and phonon absorption (emission). $|[l_z(q)]_{\gamma\alpha}|^2$ means that the implicit state is coupled with the final up-spin state by a phonon with a wave vector q. $\Delta^{(-+)}_{\alpha\gamma}(+\omega_q)$ means that the energy of the implicit state with up spin ($E_{\gamma+}$) is determined by the energy of the initial state with down spin ($E_{\alpha-}$), photon energy ($\hbar\omega$), and phonon energy ($\hbar\omega_q$). Hence, energy conservation can be satisfied, i.e., $E_{\alpha-}+\hbar\omega+\hbar\omega_q = E_{\gamma+}$.

The fifth term (E in Fig. 1) in Eq. (26), which is a spin conserving process, corresponds to an implicit transition between the implicit state with an up spin ($\gamma+$ state) and the final state with an up spin ($\alpha+$ state). The other terms in Eq. (26) can be interpreted in a similar manner. Therefore, the net transition from the initial state with the down spin to the final state with the up spin occurs through implicit transitions including the spin flip and conserving processes, and the implicit state is coupled with the initial or final states. The result could be represented in a diagram because the lineshape function contained the energy denominator, population and interaction factors properly.

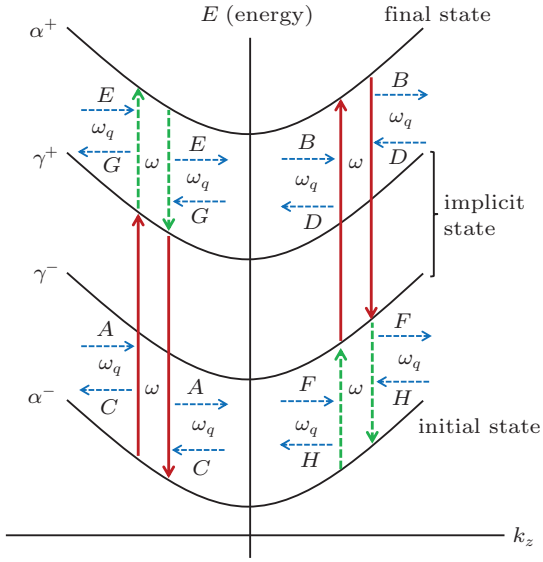


Fig. 1. (color online) All possible transition processes in Eq. (26) are depicted schematically. The vertical red solid and green dotted lines correspond to the spin flip and conserving processes, respectively.

4.2. Electron spin resonance

In this section, the lineshift term is neglected, as $\mathrm{Re}\{\Gamma_\alpha(\omega)\}$ is negligible in comparison with $E_+ - E_-$ because a very weak scattering effect is considered and the approximation that $\mathrm{Im}\{\Gamma_\alpha(\omega)\} \approx \mathrm{Im}\{\Gamma_\alpha(E_{+-})\}$ is adopted because it is a very slowly varying function of ω near the resonance point, $\hbar\omega = E_+ - E_-$. With these approximations, $\Delta^{(-+)}_{\beta\alpha}(\pm\omega_q) = \delta(E_\beta - E_\alpha \pm \hbar\omega_q)$ and $\Delta^{(c)}_{\beta\alpha}(\pm\omega_q) = \delta(E_{\beta+} - E_{\alpha-} \pm \hbar\omega_q)$, and the matrix elements in Eqs. (26) are given as follows:

$$\begin{aligned}
[l_z(q)]_{\alpha\beta} &= -l_a\hbar D_q \delta_{k_{yz\alpha},k_{yz\beta}+q_{yz}} \frac{1}{r_0}\sqrt{\frac{n_\beta}{2}} \\
&\quad \times J_{n_\alpha,n_\beta-1}(x_{c\alpha},q_x,x_{c\beta})(q_y - \mathrm{i}q_x) \\
&\quad + l_a\hbar D_q \delta_{k_{yz\alpha},k_{yz\beta}+q_{yz}} \frac{1}{r_0}\sqrt{\frac{n_\beta+1}{2}} \\
&\quad \times J_{n_\alpha,n_\beta+1}(x_{c\alpha},q_x,x_{c\beta})(q_y + \mathrm{i}q_x), \qquad (28) \\
[l^+(q)]_{\alpha\beta} &= \mathrm{i}l_a\hbar D_q k_{z\beta}\delta_{k_{yz\alpha},k_{yz\beta}+q_{yz}} \\
&\quad \times J_{n_\alpha,n_\beta}(x_{c\alpha},q_x,x_{c\beta})(q_y - \mathrm{i}q_x) \\
&\quad - \frac{\mathrm{i}\hbar}{r_0} l_a D_q q_z \sqrt{2(n_\beta+1)}\,\delta_{k_{yz\alpha},k_{yz\beta}+q_{yz}} \\
&\quad \times J_{n_\alpha,n_\beta+1}(x_{c\alpha},q_x,x_{c\beta}). \qquad (29)
\end{aligned}$$

Here, $l_a \equiv \hbar/4m_e^2c^2$, $\delta_{k_{yz\alpha},k_{yz\beta}+q_{yz}} \equiv \delta_{k_{y\alpha},k_{y\beta}+q_y}\delta_{k_{z\alpha},k_{z\beta}+q_z}$, and $J_{n,n'}(x_c,\pm q_x,x_c') \equiv \int_{-\infty}^{\infty} \mathrm{d}x\phi_n^*(x)\exp(\pm\mathrm{i}q_x x)\phi_{n'}(x)$ can be calculated as follows:

$$\begin{aligned}
&J_{n,n'}(x_c,\pm q_x,x_c') \\
&= \sqrt{\frac{n_<!}{n_>!}}\left(\frac{x_< - x_> \pm \mathrm{i}q_x r_0^2}{\sqrt{2}r_0}\right)^{n_>-n_<} \\
&\quad \times \mathrm{L}_{n_<}^{(n_>-n_<)}\left[\frac{(x_c-x_c')^2 + q_x^2 r_0^4}{2r_0^2}\right] \\
&\quad \times \exp\left[-\left(\frac{x_c-x_c'}{2r_0}\right)^2 - \left(\frac{r_0 q_x}{2}\right)^2 \pm \frac{\mathrm{i}q_x(x_c+x_c')}{2}\right], \qquad (30)
\end{aligned}$$

where $n_>$ ($n_<$) $= \max(\min)\{n,n'\}$, $t \equiv \hbar(q_x^2+q_y^2)/2eB$, and $\mathrm{L}_n^{(m)}(t)$ is the associated Laguerre polynomial. The absolute square of Eq. (30) given by

$$|J_{n,n'}(x_c,q_x,x_c')|^2 = \frac{n_<!}{n_>!}t^{n_>-n_<}\mathrm{e}^{-t}\left[\mathrm{L}_{n_<}^{(n_>-n_<)}(t)\right]^2 \qquad (31)$$

is needed to calculate Eq. (25) numerically.

5. Numerical results

The ESR peaks in silicon are calculated numerically for $n_\alpha = 0$ at the subband edge ($k_{z\alpha} = 0$) in the quantum limit. Then, only the cases for $n_\gamma = 0$ and $n_\gamma = 1$ need to be considered for the implicit transition terms appearing in Eq. (26). Note that the magnetic field B is changed instead of frequency ω because the experiment is performed in this way.

The energies of the acoustic and optical deformation phonons, $\hbar\omega_q$ and $\hbar\omega_l$, and the Fermi distribution function, $f(E_{\alpha,s_\alpha})$, for electrons in silicon are given by $\hbar\omega_q = \hbar v_s q$, $\hbar\omega_l = 0.063$ eV, and $f(E_{\alpha,s_\alpha}) = [1+\exp\{(E_{\alpha,s_\alpha}-E_F)/k_BT\}]^{-1}$, respectively. Here, v_s is the speed of sound, E_{α,s_α} is the same as that given in Eq. (11) and the Fermi energy E_F is given by[33] $E_F = E_g(T)/2 - (3/4)k_BT\ln(m_h/m_e)$, where m_h is the effective mass of a hole and $E_g(T) = E_g(0) - \alpha T^2/(T+\beta)$, with $E_g(0)$ being the energy gap at zero temperature. The physical constants for silicon are as follows:[34,35] $m_e = 0.33m_0$, $m_h = 0.53m_0$ where

m_0 is the free electron mass, $v_s = 9030$ m/s, $E_g = 1.17$ eV, $\rho_m = 2340$ kg/m^3, $\alpha = 4.73 \times 10^{-4}$ eV/K, and $\beta = 636$ K.

5.1. ESR profile

Figure 2 shows the magnetic field dependence of the magnetic susceptibility in silicon for $f = 30$ GHz and $P_{ad} = 1 \times 10^8$ eV, which was drawn from Eq. (25) using Eqs. (26) and Eqs. (28)–(31). Both the height and width of the susceptibility increase with temperature. The increases in the height and width are attributed to increases in the electron population and the number of phonons with temperature, respectively. The increases in the width with temperature agree with the results reported by Yafet.[20] For the relaxation time T_1, which is related to the linewidth by Eq. (1), Yafet presented $T_1 \propto T^{-3.5}$ when the band edge is at $\boldsymbol{k} = 0$ or at $\boldsymbol{K}_n$ as in germanium, where $\boldsymbol{K}_n$ is the reciprocal lattice vector and $T_1 \propto T^{-2.5}$ when the band edge is not at $\boldsymbol{k} = 0$ or $\boldsymbol{K}_n$ as in silicon. Figure 3 shows that the width increases with increasing magnetic field. The graph for $f = 45$ GHz was moved to the left by 1770 Gs (1 Gs $= 10^{-4}$ T) to be compared with the result for $f = 30$ GHz. This also agrees with the result reported by Yafet, $T_1 \propto B^{-2.5}$, in the high field limit.

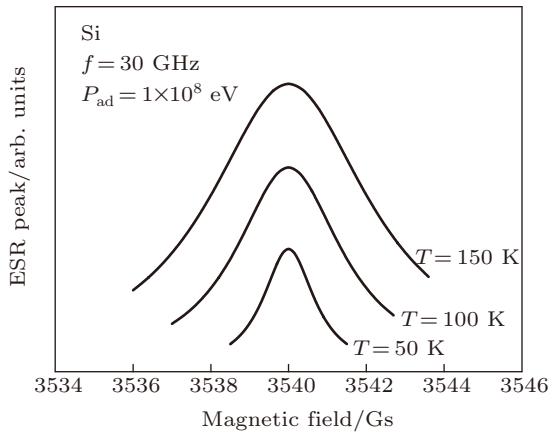


Fig. 2. The peaks of electron spin resonance at 50, 100, and 150 K in silicon for a frequency of 30 GHz and for $P_{ad} = 1 \times 10^8$ eV.

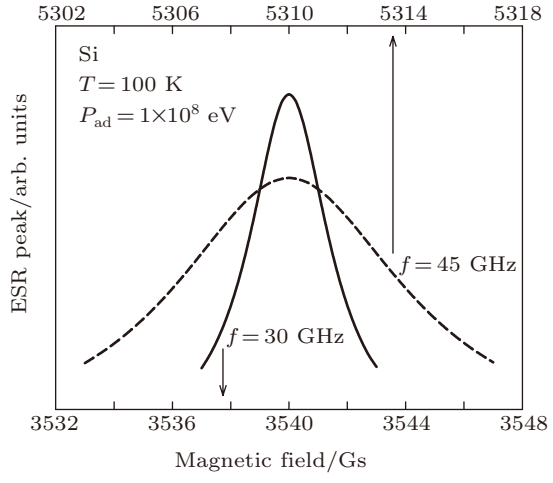


Fig. 3. The electron spin resonance peaks for frequencies of 30 GHz and 45 GHz in silicon at 100 K and for $P_{ad} = 1 \times 10^8$ eV.

5.2. Temperature dependence of T_1

Figure 4 shows the temperature dependence of the electron spin relaxation times by the acoustic and optical deformation potential scatterings in silicon for $f = 30$ GHz, $P_{ad} = 1.4 \times 10^7$ eV, and $P_{od} = 4.0 \times 10^{17}$ eV/m. The relaxation time by acoustic deformation potential scattering, T_1^{ad}, is proportional to $T^{-1.03}$ and that by optical deformation potential scattering, T_1^{od}, is proportional to $T^{-3.9}$, i.e, the relaxation times for both cases decrease with temperature T in a different manner. The decrease can be interpreted as due to an increase of the number of phonons with temperature. Note that the relaxation time is proportional to the inverse of the relaxation rate, which increases with increasing electron–phonon interaction and the interaction increases with increasing the number of phonons. The electron spin is scattered mainly by acoustic deformation potential at low temperature and optical deformation potential at high temperature. The decrease of the relaxation time with temperature agrees with the result of Yafet.[20] Yafet presented $T_1 \propto T^{-3.5} \sim T^{-2.5}$ in semiconductors. The results of others[21–25] showed similar tendencies.

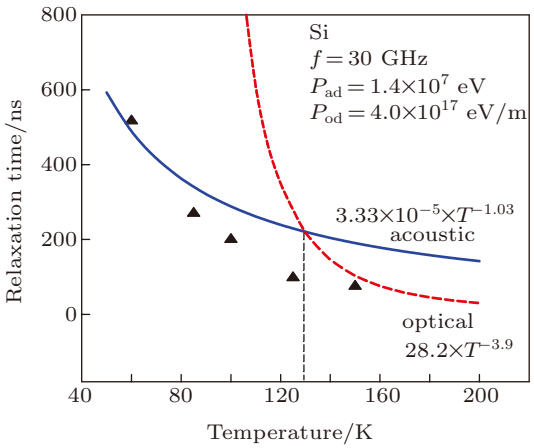


Fig. 4. (color online) The temperature dependence of the electron spin relaxation time by the acoustic (blue solid line) and optical (red short-dash line) deformation potential scatterings in silicon for $f = 30$ GHz, $P_{ad} = 1.4 \times 10^7$ eV, and $P_{od} = 4.0 \times 10^{17}$ eV/m. The black triangles are the result of Huang *et al.*[29].

Figure 5 shows that the temperature dependence of the total relaxation time in silicon for $f = 30$ GHz, $P_{ad} = 1.4 \times 10^7$ eV, and $P_{od} = 4.0 \times 10^{17}$ eV/m where Matthiessen's rule[30] is adopted to add the acoustic and optical deformation contributions to the total spin relaxation time (T_1^{tot}) as follows: $1/T_1^{tot} = 1/T_1^{ad} + 1/T_1^{od}$. The numerical result (red circles) nearly agrees with the result (black triangles) by Huang *et al.*[29] but it cannot be fitted by a curve. It can be fitted by two curves, one decreases with temperature as $T_1 \propto T^{-1.07}$ at low temperatures and is mainly affected by acoustic deformation potential scattering, and the other decreases with temperature as $T_1 \propto T^{-3.3}$ at high temperatures and is mainly affected by optical deformation potential scattering (Table 1). This means that electrons are scattered by the acoustic deformation potential at temperatures below about $T = 130$ K and the optical deformation potential at temperatures above about $T = 130$ K (see Fig. 4).

Table 1. The temperature and magnetic field dependence of the relaxation times in Si [T_1: relaxation time, T: temperature, B: magnetic field].

Temperature	Present	Yafet[20]
Low	$T_1 \propto T^{-1.07}$ (at 0.354 T) $T_1 \propto B^{-2.7}$ (at 100 K)	$T_1 \propto T^{-2.5} \sim T^{-3.5}$
High	$T_1 \propto T^{-3.3}$ (at 0.354 T) $T_1 \propto B^{-2.3}$ (at 150 K)	$T_1 \propto B^{-2.5} \sim B^{-3.0}$

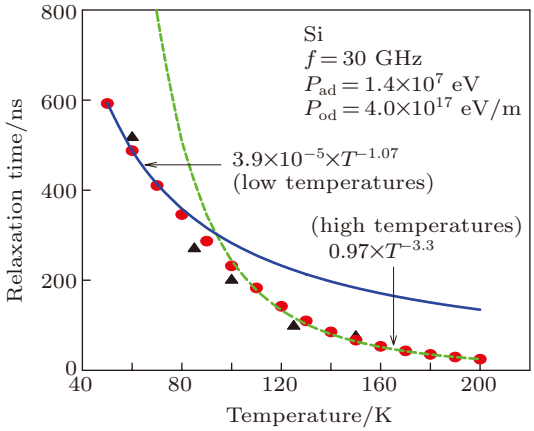


Fig. 5. (color online) The temperature dependence of the total electron spin relaxation time (red circles) in silicon for $f = 30$ GHz, $P_{ad} = 1.4 \times 10^7$ eV, and $P_{od} = 4.0 \times 10^{17}$ eV/m. The black triangles are the result of Huang *et al.*[29]

5.3. Magnetic field dependence of T_1

Figures 6 and 7 show the magnetic field dependence of the electron spin relaxation time at 100 K and 150 K, respectively, in silicon for $P_{ad} = 1.4 \times 10^7$ eV and $P_{od} = 4.0 \times 10^{17}$ eV/m. Figure 6 shows that the relaxation time decreases with magnetic field B ($T_1 \propto B^{-2.7}$) and the acoustic deformation potential is the main scattering mechanism. Figure 7 shows that the optical deformation potential is the main scattering mechanism and the relaxation time decreases with magnetic field B ($T_1 \propto B^{-2.3}$) (Table 1). These agree with the result of Yafet, $T_1 \propto B^{-2.5} \sim B^{-3.0}$.

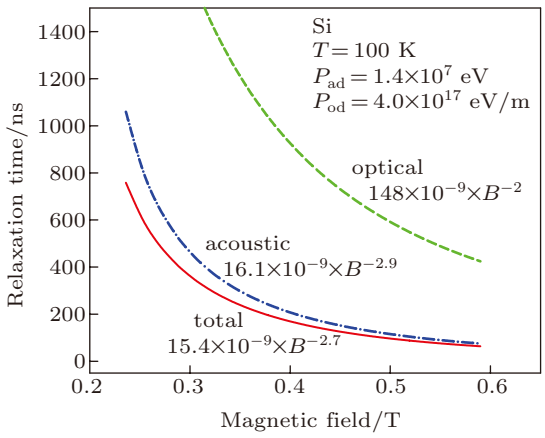


Fig. 6. (color online) The magnetic field dependence of the electron spin relaxation times at 100 K in silicon for $P_{ad} = 1.4 \times 10^7$ eV and $P_{od} = 4.0 \times 10^{17}$ eV/m.

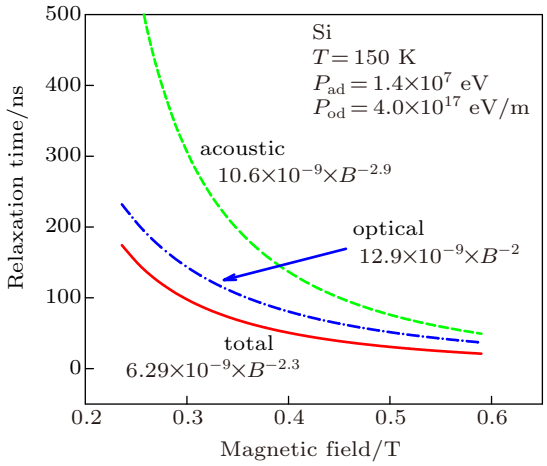


Fig. 7. (color online) The magnetic field dependence of the electron spin relaxation time at 150 K in silicon for $P_{ad} = 1.4 \times 10^7$ eV and $P_{od} = 4.0 \times 10^{17}$ eV/m.

6. Conclusions

This paper reported a new method for deriving the magnetic susceptibility for a system of electrons interacting with phonons through phonon-modulated spin–orbit coupling using the PR method. The lineshape function in the magnetic susceptibility included the population factors properly as well as the energy denominator factors enforcing energy conservation and the interaction factors coupling the implicit state with the initial or final states. Therefore, the phonon emissions and absorptions as well as the photon absorptions and emissions in all electron transition processes could be explained in an organized manner and the result could be represented diagrammatically, through which a physical model of the quantum dynamics of electrons in a solid could be obtained.

The electron spin relaxation time in silicon decreased with temperature as $T_1 \propto T^{-1.07}$ at low temperatures and $T_1 \propto T^{-3.3}$ at high temperatures. It means that the acoustic and optical deformation phonons are the main scatterers at low and high temperatures, respectively. It also turned out that the magnetic field dependence of the relaxation time was $T_1 \propto B^{-2.7}$ at 100 K and $T_1 \propto B^{-2.3}$ at 150 K, which nearly agreed with the result of Yafet.[20] In conclusion, it must be emphasized that a physically acceptable and generally applicable theory can be obtained using the PR method. It is expected that this method can be applied to electron systems interacting with piezoelectric and polar optical phonons as well as impurities in the materials such as graphite, diamond, and GaAs. This will be studied in the future.

References

[1] Datta S and Das B 1990 *Appl. Phys. Lett.* **56** 665
[2] Kane B E 1998 *Nature* **393** 133
[3] Nakamura Y, Pashkin Yu A and Tsai J S 1999 *Nature* **398** 786
[4] Wolf S A, Awschalom D D, Buhrman R A, Daughton J M, von Molnár S, Roukes M L, Chtchelkanova A Y and Treger D M 2001 *Science* **294** 1488
[5] Žutić I, Fabian J and Sarma S D 2004 *Rev. Mod. Phys.* **76** 323
[6] Yuan X B, Ren J F and Hu G C 2012 *Chin. Phys. Lett.* **29** 067501
[7] Hao Y F 2013 *Chin. Phys. B* **22** 017102

[8] Li S F, He P, Cheng C Y, Zhou S M and Lai T S 2014 *Chin. Phys. Lett.* **31** 017502
[9] Tyryshkin A M, Lyon S A, Astashkin A V and Raitsimring A M 2003 *Phys. Rev. B* **68** 193207
[10] Žutić I, Fabian J and Erwin S C 2006 *Phys. Rev. Lett.* **97** 026602
[11] Žutić I and Fabian J 2007 *Nature* **447** 268
[12] Appelbaum I, Huang B and Monsma D J 2007 *Nature* **447** 295
[13] Dash S P, Sharma S, Patel R S, de Jong M P and Jansen R 2007 *Nature* **462** 491
[14] Lepine D J 1970 *Phys. Rev. B* **2** 2429
[15] Matsunami J, Ooya M and Okamoto T 2006 *Phys. Rev. Lett.* **97** 066602
[16] Fabian J, Matos-Abiague A, Ertler C, Stano P and Žutić I 2007 *Acta Phys. Slovaca* **57** 565
[17] Schlegel C, van Slageren J, Timco G, Winpenny R E P and Dressel M 2011 *Phys. Rev. B* **83** 134407
[18] Fábián G, Dóra B, Antal Á, Szolnoki L, Korecz L, Rockenbauer A, Nemes N M, Forró L and Simon F 2012 *Phys. Rev. B* **85** 235405
[19] Elliott R J 1954 *Phys. Rev.* **96** 266
[20] Yafet Y 1963 *Solid State Physics*, Vol. 14, ed. Seitz F and Turnbull D (New York : Academic Press) Chap. 7
[21] Restrepo O D, Varga K and Pantelides S T 2009 *Appl. Phys. Lett.* **94** 212103
[22] Restrepo O D and Windl W 2012 *Phys. Rev. Lett.* **109** 166604
[23] Cheng J L, Wu M W and Fabian J 2010 *Phys. Rev. Lett.* **104** 016601
[24] Li P and Dery H 2011 *Phys. Rev. Lett.* **107** 107203
[25] Tang J M, Collins B T and Flatte M E 2012 *Phys. Rev. B* **85** 045202
[26] Kang N L and Choi S D 2008 *J. Math. Phys.* **49** 073501
[27] Kang N L and Choi S D 2010 *J. Phys. A: Math. Theor.* **43** 165203
[28] Kang N L and Choi S D 2012 *AIP Advances* **2** 012162
[29] Huang B, Monsma D J and Appelbaum I 2007 *Phys. Rev. Lett.* **99** 177209
[30] Mahan G D 2000 *Many-Particle Physics* (New York: Plenum)
[31] Kawabata A 1970 *J. Phys. Soc. Jpn.* **29** 902
[32] Ferry D K 1991 *Semiconductors* (New York: Macmillan) Chap. 7
[33] Varshni V P 1967 *Physica* **34** 149
[34] Wolfe C M and Stillman G E 1989 *Physics Properties of Semiconductors* (NJ: Prentice-Hall)
[35] Chuang S L 1995 *Physics of Optoelectronic Devices* (New York: Wily)